Alignment of Cortical Vessels viewed through the Surgical Microscope with Preoperative Imaging to Compensate for Brain Shift

Nazim Haouchine, Parikshit Juvekar, Alexandra Golby, William M Wells, Stéphane Cotin, Sarah Frisken

Alignment of Cortical Vessels viewed through the Surgical Microscope with Preoperative Imaging to Compensate for Brain Shift

Nazim Haouchine[a,b], Parikshit Juvekar[a,c], Alexandra Golby[a,c], William M. Wells III[a,b], Stephane Cotin[d], Sarah Frisken[a,b]

[a] Harvard Medical School, Boston, MA, USA;
[b] Department of Radiology, Brigham and Women's Hospital, Boston, MA, USA;
[c] Department of Neurosurgery, Brigham and Women's Hospital, Boston, MA, USA;
[d] Inria, Strasbourg, France

ABSTRACT

Brain shift is a non-rigid deformation of brain tissue that is affected by loss of cerebrospinal fluid, tissue manipulation and gravity among other phenomena. This deformation can negatively influence the outcome of a surgical procedure since surgical planning based on pre-operative image becomes less valid. We present a novel method to compensate for brain shift that maps preoperative image data to the deformed brain during intra-operative neurosurgical procedures and thus increases the likelihood of achieving a gross total resection while decreasing the risk to healthy tissue surrounding the tumor. Through a 3D/2D non-rigid registration process, a 3D articulated model derived from pre-operative imaging is aligned onto 2D images of the vessels viewed through the surgical miscroscopic intra-operatively. The articulated 3D vessels constrain a volumetric biomechanical model of the brain to propagate cortical vessel deformation to the parenchyma and in turn to the tumor. The 3D/2D non-rigid registration is performed using an energy minimization approach that satisfies both projective and physical constraints. Our method is evaluated on real and synthetic data of human brain showing both quantitative and qualitative results and exhibiting its particular suitability for real-time surgical guidance.

Keywords: Brain Shift, Non-rigid registration, Biomechanical Modelling, Augmented Reality, Image-guided Neurosurgery

1. INTRODUCTION

Intra-operative brain shift is a well-known phenomenon that describes movement and deformation of the brain in terms of its anatomical and physiological position in the skull during neurosurgery.[1,2] Several methods have been proposed in the literature to estimate brain shift using pre-operative and intra-operative image data using various types of imaging techniques such as Cone-Beam Computed Tomography,[3] B-mode ultra-sound[4],[5] Doppler ultra-sound,[6] Laser range scanner[7] or intra-operative MRI.[8] Most of these methods are solely based on image processing since they do not involve additional pre-operative preparation. In Filipe *et al.*,[9] a non-rigid deformation pipeline using superficial vessel centerlines have been proposed. The method uses Thin Plate Spline (TPS) to compute the deformation and Coherent Point Drift (CPD) for centerline registration. More advanced methods than CPD have been evaluated for the non-rigid registration stage. In Bayer *et al.*,[10] a Hybrid Mixture Model is used and outperforms the classic CPD approach. This method is combined with TPS-like interpolation to generate a dense deformation field. In Machado *et al.*,[11] a feature-based active registration method is proposed. 3D SIFT-Rank is used to find correspondences and estimate dense mappings throughout the image. This method was shown to be robust in clinical routines and can benefits from additional landmarks selected by surgeons thanks to an active framework.[12] Instead of using geometric models such as TPS to compute deformation, several approaches proposed to use biomechanical models.[7,13–17] Recently, Morin *et al.*[14] measured brain shift at the brain surface and sub-surface vessels using intraoperative doppler-based ultrasound and then used physics-based models to propagate the deformation to regions of the brain where arteries are not present. In Sun *et al.*[7] pre-computed atlases of the brain are used to simulate brain shift following a sparse set if image-points extracted from the cortical brain surface using an optically tracked portable laser range scanner. In Luo *et al.*[18] an optically tracked stylus is used to identify cortical surface vessel features; these features are integrated in a model-based workflow to estimate brain shift correction after craniotomy and dural opening. Stereovision has been used as a means to capture the shape of the exposed brain and infer the deformation caused by brain shift. The method proposed by Mohammadi *et al.*[17] used a projection-based stereovision process to map brain surface with a pre-operative finite element model. The projection of a pre-defined pattern permits to recover the 3D shape of the

brain that is coupled with ultrasound imaging to perform a non-rigid registration. Ji *et al.*[19] proposed to combine optical flow and stereovision constraints to reconstruct a 3D dense brain surface at two different surgical stages leading to obtain an undeformed and deformed surface. A non-rigid registration between the underformed and deformed surface is used to determine the deformation of the exposed brain surface during surgery.

In this paper we propose a vessel-based method to register pre-operative scans onto intra-operative images captured through the surgical microscope. Our method uses cortical vessels at the surface since images of the brain surface from the craniotomy are available in real-time through the oculars of the microscope (or possibly a ceiling mounted camera) while intra-operative ultra sound and intra-operative MRI both require significant cost and time. In comparison to previous methods, we rely solely on a single image acquired from the surgical microscope, to avoid tedious calibration of the stereo camera, laser range finder or optical stylus, which makes previous approaches impractical in most hospital settings. This narrows down our problem to a 3D/2D non-rigid registration between undeformed 3D centerlines and deformed 2D centerlines that can be solved by satisfying a combination of physical and projective constraints. The surface deformation estimated by this method is then propagated to the rest of the brain using a biomechanical model, built from pre-operative MRI scans, that has proven to be fast and reliable to model the brain tissue and its inner structures.[20,21]

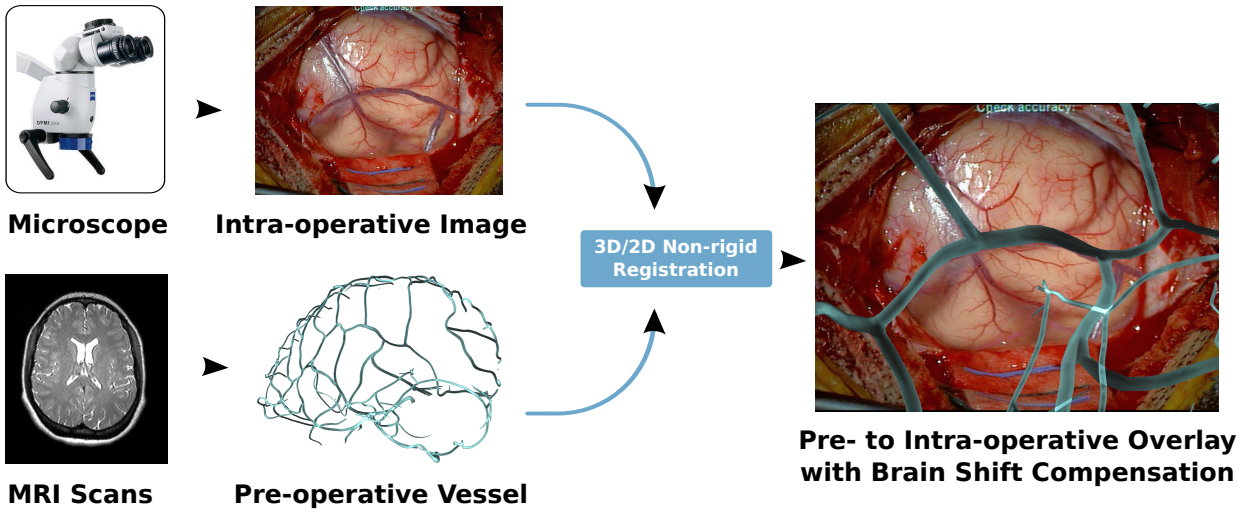

Figure 1: Overview of our pipeline: inputs of our system consist of a single intra-operative image acquired from the surgical microscope and a model of brain surface derived from the pre-operative MRI. A 3D/2D non-rigid registration method is applied to align the vessels. This alignment is propagated to the rest of the brain using a biomechanical model to provide a 3D model of brain shift.

2. METHODS

2.1 Method overview

Our approach updates the pre-operative neurosurgical plan (particularly the tumor position) by taking into account the intra-operative brain shift. As shown in the pipeline of figure 1, at any time t, inputs to our registration system include a single monocular image, $\mathscr{I}$, acquired intra-operatively via the surgical microscope and a 3D model of the cortical vessels, $\mathscr{V}$, derived from the pre-operative MRI. A 3D/2D non-rigid registration method is applied to align the vessels to the image. This registration deforms the vessels while preserving its physical consistency. This deformation estimates a shift of the whole brain (global) from a sub-part of the brain surface (local). The local deformation is converted to a global deformation using a biomechanical model that propagates the location deformation of cortical veins to deep structures including vessels and the tumor.

2.2 Data processing and problem formulation

The first stage of our pipeline is processing the input intra-operative image $\mathscr{I}$ and pre-operative vessels $\mathscr{V}$. We chose to rely on vascular network graphs (or centerlines) to perform our non-rigid registration (see figure 2). Indeed, centerlines represent an effective shape abstraction over using the complete vascular network and can be manipulated more easily.

For this preliminary study, extracting centerlines from $\mathscr{I}$ is done manually, by interactively selecting a set of points representing the starting and ending points of vessel segments. More advanced methods exist, either supervised or unsupervised[22,23] and could be easily plugged in our pipeline. We denote $\mathbf{U} = \{u_j \in \mathbb{R}^2\}$, the set of 2D points corresponding to the intra-operative centerlines. Extracting the centerlines from $\mathscr{V}$ is done by first segementing the MRI scans and building a triangulated surface mesh of the vessels. This mesh is then iteratively thinned using mean curvature skeletonization[24] to obtain the final centerlines that we denote $\mathbf{V} = \{v_i \in \mathbb{R}^3\}$.

Our goal is to find the transformation function Φ so that $\mathbf{U} = \Phi_{(\Pi,\mathbf{R},\mathbf{t},\delta\mathbf{u})}(\mathbf{V})$ where Π is the camera matrix that transforms camera coordinates to world coordinates, $\mathbf{R}$ and $\mathbf{t}$ are respectively the rotation and translation matrices representing rigid transformation components and $\delta\mathbf{u}$ is the non-rigid transformation component.

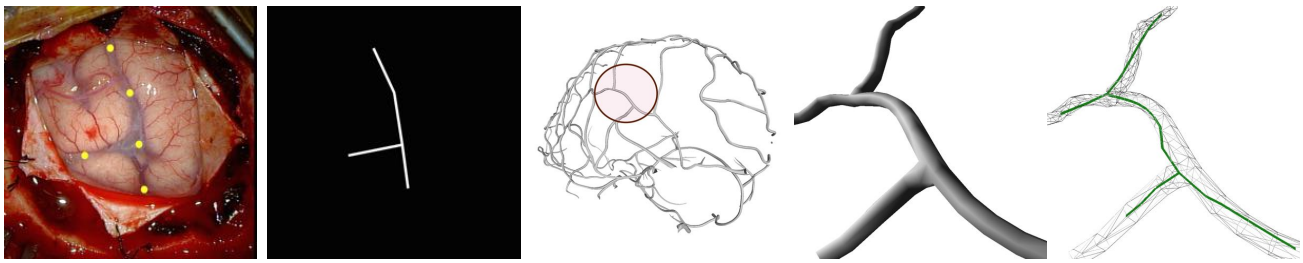

(a) (b) (c) (d) (e)

Figure 2: Input data processing: (a) interactive points selection, (b) centerlines between starting and ending points, (c) pre-operative vessel with region of interest, (d) zoom on the region on interest, (e) centerline extraction using mean curvature skeletonization.

2.3 Modelling the vessels and its surrounding tissues

Let $\mathbf{S}$ be a 3D triangulated surface mesh of the brain generated from pre-operative MRI scans that includes the parenchyma, internal structures such as vessels or tumors, and constraints from surrounding anatomical information such as the skull.[21] The mesh $\mathbf{S}$ allows us to build a physical model incorporating tissue properties and biomechanical behavior (see Figure 3). This physical model is characterized by a geometry $\mathbf{S}$ and a stiffness matrix $\mathbf{K}$ that describe physical properties such as tissue elasticity, damping or viscosity. In order to account for tissue heterogeneity, the stiffness matrix of the whole brain is a mechanical composition of paranchyma and vessel stiffness properties. This mechanical coupling permits the propagation of vessel deformation to the paranchyma and the tumor. In practice, the global stiffness matrix is built so that each element of the parenchyma model that intersects a vessel centerline has a higher stiffness.

The deformation is specified by its stress-strain relationship. The brain deformation is computed using a non-linear geometric finite element method, with a linear constitutive law,[25] where the finite element model is meshed with linear

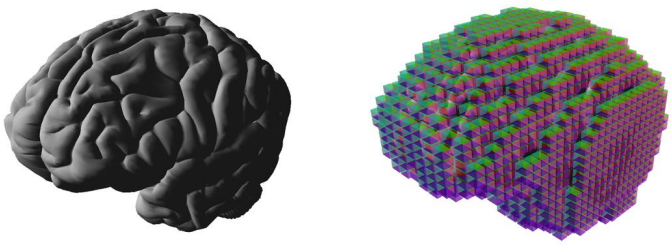

(a) (b)

Figure 3: Constructing the biomechanical model: (a) a 3D surface model $\mathbf{S}$ derived from the preoperative MRI scan and (b) a 3D hexahedral volume model generated using the geometrical properties and the stiffness matrix

hexahedrons. This allows for rotation in the model, while relying on a linear expression of the stress-strain relationship. The equation relating the external forces $\mathbf{f}$ to the nodal displacements $\mathbf{x}$ can be written as $\mathbf{f} = \mathbf{K}(\mathbf{x})\delta\mathbf{x}$.

2.4 Energy-based Non-rigid Registration

As most of the registration algorithms, our non-registration has an intialization phase. This consists of a rigid alignment, done manually, that permits to initialize the rotation matrix $\mathbf{R}$ and translation vector $\mathbf{t}$. With $\mathbf{R}$ and $\mathbf{t}$ set, a correspondences vector $\mathbf{C} = \{c_i \in \mathbb{N}\}$ can be built. This vector is built so that if a source point v_i corresponds to a target point u_j then $c_i = j$ for each point of the source set. Having the biomechanical model on one hand and the set of correspondences $\mathbf{C}$ on the other hand, we can update the pre-operative 3D mesh $\mathbf{S}$ by registering the pre-operative centerlines $\mathbf{V}$ with the intra-operative centerlines $\mathbf{U}$ that minimizes the physical energy of the biomechanical model. This leads to the following energy minimization expression:

$$\min_{\delta\mathbf{u}} \left(\overbrace{\frac{1}{2}\|\delta\mathbf{u}^\top \mathbf{K}\delta\mathbf{u}\|}^{\text{Physical consistency}} + \overbrace{\sum_{i \in n_C} \frac{1}{2}\kappa\|v_i - \Pi u_{c_i}\|^2}^{\text{Image fitting}} \right) \tag{1}$$

where κ is the stiffness coefficient that ties the source and target centerlines to compute the bending energy. Note the subscript c_i that denotes the correspondence indices between the two point sets. The image fitting term can be considered as sightlines coming from the camera position to the 2D centerlines that enforces the physical model to fit the image.

3. RESULTS

3.1 Simulated Data

We tested our method on synthetic data of a complete human brain. The vessel centerlines were extracted from the vessels and linearly down-sampled to permit a point-to-point vessel matching. The number of centerlines nodes after down-sampling is 102 nodes. The biomechanical brain model is derived from the triangular mesh using Delaunay volume triangulation. In our tests, both hemispheres are meshed with approximately 1000 tetrahedrons. The stiffness matrix is built with a Young's modulus E set to 3000 Pa and Poisson's ratio to 0.45. We used the SOFA framework to build the biomechanical model.[26]

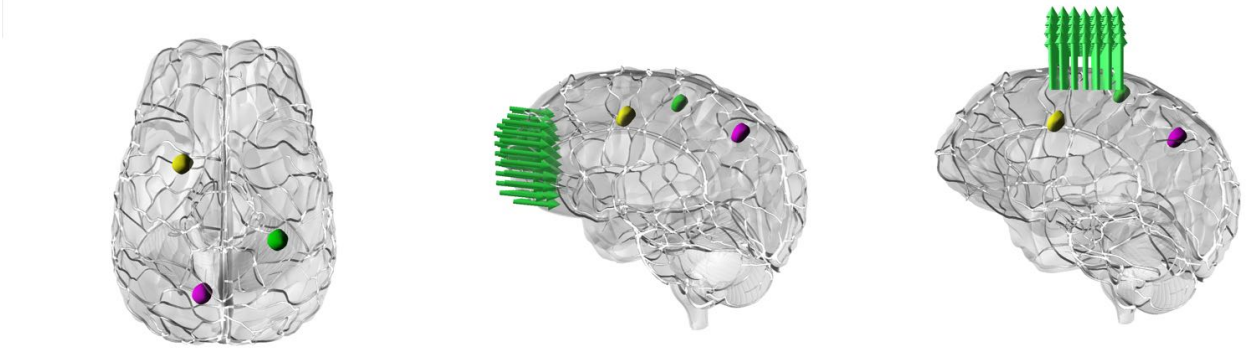

(a) (b) (c)

Figure 4: Synthetic data experiments: (a) tumor positions inside the brain, tumor 1 is in purple, tumor 2 is in yellow and tumor 3 is in green. (b) Simulated force applied to mimic brain sliding towards the back of the skull. (c) Simulated force applied to mimic protrusion deformation that occurs during craniotomy.

We quantitatively evaluated our method by measuring the registration error on tumors. We considered 3 tumors at different locations close to the surface (see figure 4-a). We simulated the brain shift under two different scenarios: the

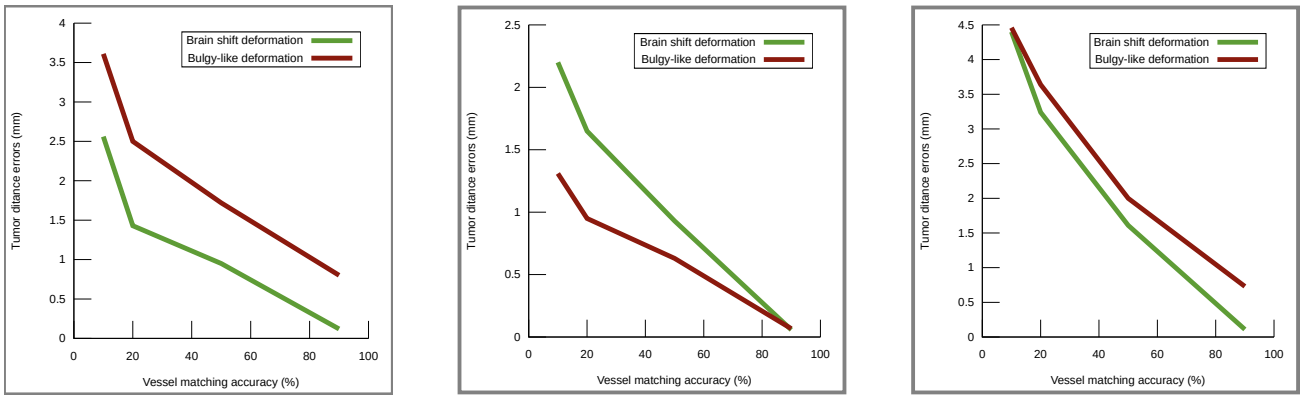

(a) Tumor 1 (b) Tumor 2 (c) Tumor 3

Figure 5: Quantitative evaluation of registration error on tumors.

first one mimicked the brain sliding towards the back of the skull under gravity as illustrated in figure 4-b and the second simulates a protrusion deformation that can occur due to brain swelling after the craniotomy as illustrated in figure 4-c. From the simulated data we extracted the 3D vessel centerlines to perform the matching where we added Gaussian noise with a standard deviation of 5 mm and a 5 clustering decimation on a subset of points composing the centerlines. We calculated the error as the Euclidean distance between the center of mass of the simulated tumors and the ones measured using our method. The results reported in figure 5 show the registration error for each tumor. Depending on the location of the tumors, we measured a distance error ranging from 0.63 mm to 2 mm with a vessel correspondence of 50% which corresponds to a 81% and 68% brain-shift correction respectively (The brain-shift correction is measured as the difference between the initial error and the corrected error divided by the initial error).

In addition to tumor locations, we measured the registration error on the brain surface using Hausdorff distance. As shown in Figure 6, the maximum measured Hausdorff distance was 3.2 mm with a vessel correspondence of 50%. We can also observe that gravity-induced deformation generates less errors than deformations caused by brain swelling at the site of the craniotomy.

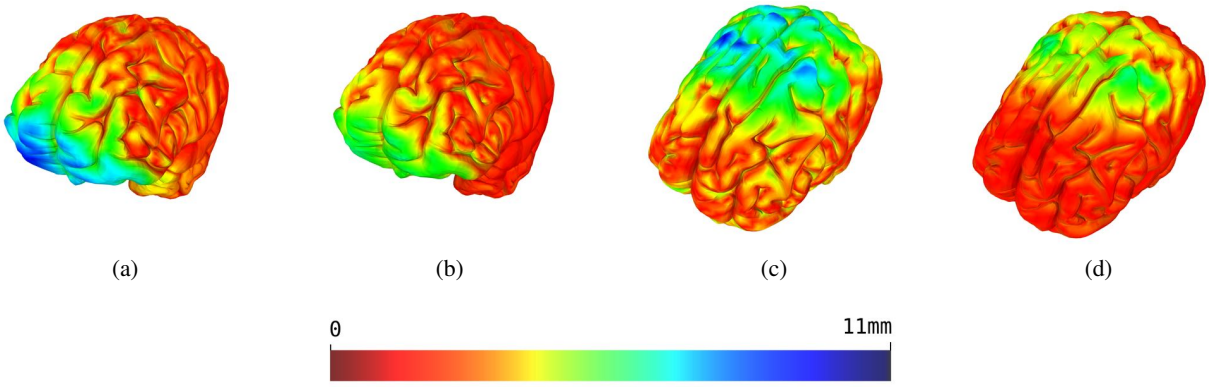

(a) (b) (c) (d)

Figure 6: Color maps corresponding to the registration errors for the simulated data experiments: (a) and (b): brain surface registration errors for gravity-induced deformation with 10% matching and 90% matching respectively, (c) and (d) brain surface registration errors for protrusion deformation with 10% matching and 90% matching respectively.

We furthermore downgraded the matching quality by decreasing the number of vessel correspondences, from 90% to 10% to demonstrate the capability of the model to interpolate deformation where no image information is available. As shown in figures 5 and 6 the registration error on the tumors and the brain surface decreases monotonically as the number of

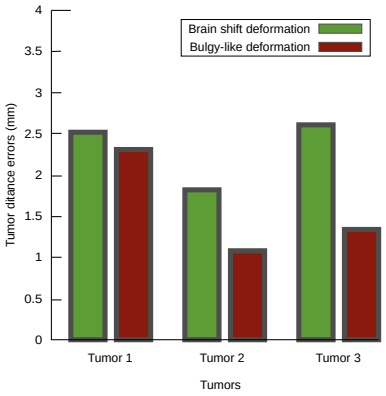

Figure 7: Registration errors on a sub part of the brain for both types of deformations.

correspondences increases. In the worst case where only 10% of the correspondences are used, we measured a maximum Euclidean distance between tumors' center of masses of 3.61 mm for tumor 1, 2.20 mm for tumor 2 and 4.46 mm for tumor 3, and a maximum Hausdorff distance of 10.19 mm for the brain surface.

We tested our method on a subset of centerlines nodes to get closer to a craniotomy case where only a small part of the brain is visible. This subset is composed of 8 nodes regularly distributed over the centerlines. We plotted in Figure 7 the actual registration error between the estimated tumors' positions and the ground truth positions for both type of deformation. The errors are more important compared to the global registration but are still acceptable with a minimal distance of 1.08 mm and a maximal distance of 2.61 mm. Tumor 2 located near the visible surface vessel subset exhibits the lowest distance errors while the tumor 3 located deeper w.r.t the selected surface shows the highest distance errors.

3.2 Real Data

We tested our method on real data using images acquired from a Carl Zeiss surgical microscope. The scope is equipped with two cameras with a video frame rate of approximately 30 frames per second. We used only the left image. The pre-operative mesh is first aligned manually on the image to obtain the rigid transform, then, the non-rigid refinement is performed, which will drive the whole brain mesh. The Figure 8 shows the non-registration process and the resulting mesh-to-image overlay.

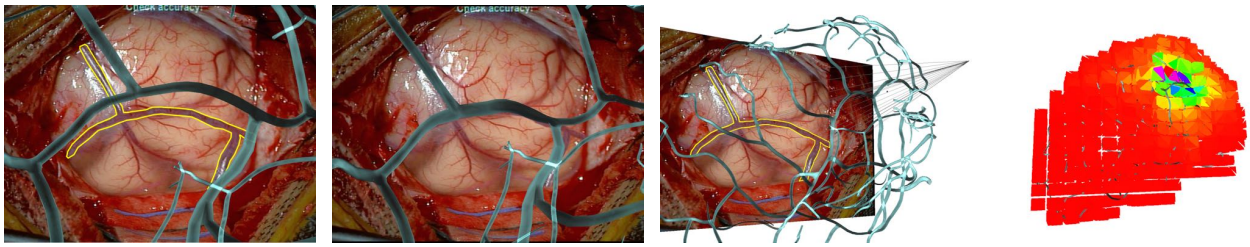

(a) (b) (c) (d)

Figure 8: Experiments using real-world data: (a) inital rigid registration, (b) non-rigid registration, (c) alternate point of view showing the 2D constraints and (d) deformation propagation onto the volume model

4. CONCLUSION

We propose a method to update pre-operative neurosurgical planning by taking into account brain deformation induced by brain shift. Our method follows a 3D/2D non-rigid process between pre-operative and intra-operative cortical vessels centerlines using a single image instead of a stereo pair. Our method shows promising results in estimating brain tumor positions subject to two common types of brain shift, a gravity-induced deformation and a protrusion deformation. In addition, our results suggest that cortical vessels can be considered as strong features to estimate brain shift deformation.

This approach can be used for neurosurgical navigation when vessels visible on the surface can be captured using a surgical microscope.

Future work will consist of extending the experiments on real data with surgical conditions and include an automated algorithm for vessels' centerlines extraction from microscopic images.

5. ACKNOWLEDGEMENTS

The authors were supported by the following funding bodies and grants: NIH: R01 EB027134-01, NIH: R01 NS049251 and BWH Radiology Department Research Pilot Grant Award.

REFERENCES

[1] Bayer, S., Maier, A., Ostermeier, M., and Fahrig, R., "Intraoperative imaging modalities and compensation for brain shift in tumor resection surgery," *International Journal of Biomedical Imaging* **2017**, 1–18 (06 2017).

[2] Miga, M. I., Sun, K., Chen, I., Clements, L. W., Pheiffer, T. S., Simpson, A. L., and Thompson, R. C., "Clinical evaluation of a model-updated image-guidance approach to brain shift compensation: experience in 16 cases," *International Journal of Computer Assisted Radiology and Surgery* **11**, 1467–1474 (Aug 2016).

[3] Pereira, V. M., Smit-Ockeloen, I., Brina, O., Babic, D., Breeuwer, M., Schaller, K., Lovblad, K.-O., and Ruijters, D., "Volumetric Measurements of Brain Shift Using Intraoperative Cone-Beam Computed Tomography: Preliminary Study," *Operative Neurosurgery* **12**, 4–13 (08 2015).

[4] Ji, S., Wu, Z., Hartov, A., Roberts, D. W., and Paulsen, K. D., "Mutual-information-based image to patient re-registration using intraoperative ultrasound in image-guided neurosurgery," *Medical Physics* **35**(10), 4612–4624 (2008).

[5] Rivaz, H. and Collins, D. L., "Deformable registration of preoperative mr, pre-resection ultrasound, and post-resection ultrasound images of neurosurgery," *International Journal of Computer Assisted Radiology and Surgery* **10**, 1017–1028 (Jul 2015).

[6] Reinertsen, I., Lindseth, F., Askeland, C., Iversen, D. H., and Unsgård, G., "Intra-operative correction of brain-shift," *Acta Neurochirurgica* **156**, 1301–1310 (Jul 2014).

[7] Sun, K., Pheiffer, T., Simpson, A., Weis, J., Thompson, R., and Miga, M., "Near real-time computer assisted surgery for brain shift correction using biomechanical models," *Translational Engineering in Health and Medicine, IEEE Journal of* **2**, 1–13 (04 2014).

[8] Kuhnt, D., Bauer, M. H. A., and Nimsky, C., "Brain shift compensation and neurosurgical image fusion using intraoperative mri: Current status and future challenges," *Critical Reviews and trade in Biomedical Engineering* **40**(3), 175–185 (2012).

[9] Marreiros, F. M. M., Rossitti, S., Wang, C., and Smedby, Ö., "Non-rigid deformation pipeline for compensation of superficial brain shift," in [*MICCAI 2013*], 141–148, Springer Berlin Heidelberg, Berlin, Heidelberg (2013).

[10] Bayer, S., Ravikumar, N., Strumia, M., Tong, X., Gao, Y., Fahrig, R., Ostermeier, M., and Maier, A., "Intraoperative brain shift compensation using a hybrid mixture model," (09 2018).

[11] Machado, I., Toews, M., Luo, J., Unadkat, P., Essayed, W., George, E., Teodoro, P., Carvalho, H., Martins, J., Golland, P., Pieper, S., Frisken, S., Golby, A., and Wells, W., "Non-rigid registration of 3d ultrasound for neurosurgery using automatic feature detection and matching," *International Journal of Computer Assisted Radiology and Surgery* **13**, 1525–1538 (Oct 2018).

[12] Luo, J., Toews, M., Machado, I., Frisken, S., Zhang, M., Preiswerk, F., Sedghi, A., Ding, H., Pieper, S., Golland, P., Golby, A., Sugiyama, M., and Wells III, W. M., "A feature-driven active framework for ultrasound-based brain shift compensation," in [*MICCAI 2018*], 30–38 (2018).

[13] Miga, M. I., "Computational modeling for enhancing soft tissue image guided surgery: An application in neurosurgery," *Annals of Biomedical Engineering* **44**, 128–138 (Jan 2016).

[14] Morin, F., Courtecuisse, H., Reinertsen, I., Lann, F. L., Palombi, O., Payan, Y., and Chabanas, M., "Brain-shift compensation using intraoperative ultrasound and constraint-based biomechanical simulation," *Medical Image Analysis* **40**, 133 – 153 (2017).

[15] Garlapati, R., Roy, A., Joldes, G., Wittek, A., Mostayed, A., Doyle, B., Warfield, S., Kikinis, R., Knuckey, N., Bunt, S., and Miller, K., "More accurate neuronavigation data provided by biomechanical modeling instead of rigid registration," *J Neurosurg* **120**, 1477–83 (06 2014).

[16] Luo, M., Larson, P. S., Martin, A. J., Konrad, P. E., and Miga, M. I., "An integrated multi-physics finite element modeling framework for deep brain stimulation: Preliminary study on impact of brain shift on neuronal pathways," in [*Medical Image Computing and Computer Assisted Intervention – MICCAI 2019*], Shen, D., Liu, T., Peters, T. M., Staib, L. H., Essert, C., Zhou, S., Yap, P.-T., and Khan, A., eds., 682–690, Springer International Publishing, Cham (2019).

[17] Mohammadi, A., Ahmadian, A., Azar, A. D., Sheykh, A. D., Amiri, F., and Alirezaie, J., "Estimation of intraoperative brain shift by combination of stereovision and doppler ultrasound: phantom and animal model study," *International Journal of Computer Assisted Radiology and Surgery* **10**, 1753–1764 (Nov 2015).

[18] Luo, M., Frisken, S. F., Narasimhan, S., Clements, L. W., Thompson, R. C., Golby, A. J., and Miga, M. I., "A comprehensive model-assisted brain shift correction approach in image-guided neurosurgery: a case study in brain swelling and subsequent sag after craniotomy," in [*Medical Imaging 2019: Image-Guided Procedures, Robotic Interventions, and Modeling*], Fei, B. and Linte, C. A., eds., **10951**, 15 – 24, International Society for Optics and Photonics, SPIE (2019).

[19] Ji, S., Fan, X., Roberts, D. W., Hartov, A., and Paulsen, K. D., "Cortical surface shift estimation using stereovision and optical flow motion tracking via projection image registration," *Medical Image Analysis* **18**(7), 1169 – 1183 (2014).

[20] Mendizabal, A., Bessard Duparc, R., Bui, H. P., Paulus, C., Peterlik, I., and Cotin, S., "Face-based smoothed finite element method for real-time simulation of soft tissue," 101352H (03 2017).

[21] Bilger, A., Dequidt, J., Duriez, C., and Cotin, S., "Biomechanical simulation of electrode migration for deep brain stimulation," in [*Medical Image Computing and Computer-Assisted Intervention – MICCAI 2011*], 339–346, Springer Berlin Heidelberg, Berlin, Heidelberg (2011).

[22] Fraz, M., Remagnino, P., Hoppe, A., Uyyanonvara, B., Rudnicka, A., Owen, C., and Barman, S., "Blood vessel segmentation methodologies in retinal images - a survey," *Comput. Methods Prog. Biomed.* **108**, 407–433 (Oct. 2012).

[23] Ding, S., Miga, M. I., Thompson, R. C., Garg, I., and Dawant, B. M., "Automatic segmentation of cortical vessels in pre- and post-tumor resection laser range scan images," in [*Medical Imaging 2009: Visualization, Image-Guided Procedures, and Modeling*], Miga, M. I. and Wong, K. H., eds., **7261**, 41 – 48, International Society for Optics and Photonics, SPIE (2009).

[24] Tagliasacchi, A., Alhashim, I., Olson, M., and Zhang, H., "Mean curvature skeletons," *Comput. Graph. Forum* **31**, 1735–1744 (Aug. 2012).

[25] Nealen, A., Müller, M., Keiser, R., Boxerman, E., and Carlson, M., "Physically based deformable models in computer graphics," *Computer Graphics Forum* **25**(4), 809–836 (2006).

[26] Faure, F., Duriez, C., Delingette, H., Allard, J., Gilles, B., Marchesseau, S., Talbot, H., Courtecuisse, H., Bousquet, G., Peterlik, I., and Cotin, S., "Sofa: A multi-model framework for interactive physical simulation," *Soft Tissue Biomechanical Modeling for Computer Assisted Surgery* , 283–321, Springer Berlin Heidelberg, Berlin, Heidelberg (2012).